Per. Mineral. (2005), *74*, 1, 55-67 http://go.to/permin

PERIODICO di MINERALOGIA
established in 1930

An International Journal of
MINERALOGY, CRYSTALLOGRAPHY, GEOCHEMISTRY, ORE DEPOSITS, PETROLOGY, VOLCANOLOGY
and applied topics on *Environment, Archaeometry* and *Cultural Heritage*

The mortars of the «Fortezza delle Verrucole - S. Romano in Garfagnana (LU)»

MARCO LEZZERINI*

Dipartimento di Scienze della Terra, Università di Pisa, Via S. Maria, 53 - 56126 Pisa (Italy)

Submitted, June 2003 - Accepted, September 2004

ABSTRACT. — Twenty-one mortar samples taken from the walls in the southwest side of the *Fortezza delle Verrucole* (IX-XVIII century) – S. Romano in Garfagnana (Lucca, Italy) – have been analysed to characterise their binder and aggregate fractions. The chemical, mineralogical, petrographic and physical data collected on the bulk mortar samples show that the stone walls were built up using different mortars. The mortars with a hydraulic-binder are prevailing on those with an air-hardening lime binder. The older mortars, coming from the walls built before the XV century, were produced mixing lime putty with locally available sands. They are characterized by a sandy aggregate with grain size from medium to very coarse and by a number of snow-white lumps, due to a not complete mixing between binder and aggregate. This last feature suggests that the mortars were prepared, as it was usual in ancient times, hand-mixing the lime putty added to the sand. Hydraulic and highly hydraulic limes and, perhaps, cement mortars were later employed during operation of renovating and restoring.

RIASSUNTO. — Ventuno campioni di malte prelevate dalle strutture murarie della porzione sud-occidentale della *Fortezza delle Verrucole* (IX-XVIII century) – S. Romano in Garfagnana (Lucca, Italy) sono stati analizzati al fine di caratterizzare il tipo di legante e di aggregato utilizzati per la loro preparazione. Dai dati chimici, minero-petrografici e fisici raccolti emerge che nelle mura difensive di questa fortezza sono state impiegate prevalentemente malte confezionate con legante idraulico e, subordinatamente, malte a base di calce aerea. Le malte più antiche, prelevate da strutture murarie già edificate nel XV secolo, sono risultate composte da grassello di calce miscelato con sabbie fluviali reperibili nelle vicinanze della costruzione. Queste malte sono caratterizzate da un aggregato sabbioso con granulometria variabile da media a grossolana e dalla presenza di numerosi grumi d'impasto che indicano una imperfetta miscelazione. Quest'ultimo aspetto suggerisce che le malte fossero preparate, come spesso accadeva in passato, miscelando a mano grassello di calce e sabbia. Calci idrauliche e, probabilmente, malte a base di cemento sono state impiegate nei lavori di restauro.

KEY WORDS: *Mortars, air-hardening binders, hydraulic binders, lumps, Fortezza delle Verrucole, S. Romano in Garfagnana, Lucca, Italy.*

INTRODUCTION

The *Fortezza delle Verrucole* (FV) is a Middle Age fortress, located on a small

* E-mail: lezzerini@dst.unipi.it

morphological high, near to the left side of the Serchio River, about 1 km NW of S. Romano in Garfagnana (Lucca province) (Fig. 1). The site morphology and the building materials available in the surroundings determined its design.

The historical, architectural and structural features point out that the construction of the FV began in IX century A.D., starting at its southwest side and making progress in subsequent stages until about the XVIII century A.D. (De Angeli *et al.*, 1998). Preliminary observations and survey of both employed building materials and stones available in the studied area indicated that the defensive walls were initially built up using pebbles coming from the Serchio River and lime mortars. Later on, natural deterioration processes and structural modifications of the defensive masonries required restoration and conservation interventions. During these interventions mortars with different binding materials, such as natural and artificial hydraulic limes, and probably cement, were used instead of the original lime mortars. Thus, the study of the binder and aggregate of mortars allows to identify older constructive phases and to contribute to their historical and material knowledge.

Chemical, mineralogical and petrographic methodologies such as optical observations, X-ray fluorescence, X-ray powder diffraction, simultaneous thermal analysis and scanning electron microprobe equipped by microanalysis system, were used to obtain a sound investigation on mortar compositions and textures. This research offers useful parameters to single out the different building phases and to evaluate the behaviour of the materials employed under the environmental conditions of the Garfagnana area.

MATERIALS AND METHODS

Sampling

Giovannetti and Notini (1998), on the basis of a late archaeological excavation campaign, split up the south western side of the fortress into some buildings that they subdivide in two groups of age respectively pre-Estense (building bodies CF200 and CF400, Fig. 1) and post-Estense (CF100 and CF300 and CF500), i.e. before and after the XV century. The excavations have also unearthed some parts of the walls that were buried for a long time. Twenty-one mortar samples were collected and selected following the information given by the above-mentioned Authors (Figure 1). Table 1 reports the places and the heights (H) over the local ground level where the samples were picked up. Negative H values mean that the sample was collected in an excavation. Sampling places numbered 1 and 2 are located in two contiguous parts of an indoor wall of the fortress. The two parts differ between them for the masonry texture and the mortar features. Three samples, at different heights on the same vertical line, have been collected in place number 3 corresponding to the internal side of the surrounding walls of the fortress. The four samples from place number 4 belong to three successive levels of mortar employed for waterproofing an underground water pipe. Samples at different heights in the building body CF300 (Giovannetti and Notini, 1998) have been collected in number 5, 6 and 7, respectively. The sample from place number 8 belongs to building body CF100 (Giovannetti and Notini, 1998).

It was not possible to collect samples from the central pre-Estense building body, the *Rocca Tonda* (CF200 in Giovannetti and Notini, 1998), because during the restoration done about ten years ago all the interstices among the building stones were filled by a recent mortar.

Analytical techniques

The macroscopic features of the mortar samples were observed with a Wild-M3C stereomicroscope. From each collected sample some parallelepipeds, with a volume of around 30 cm^3, were cut by a thin, water cooled, diamond saw thus obtaining not altered

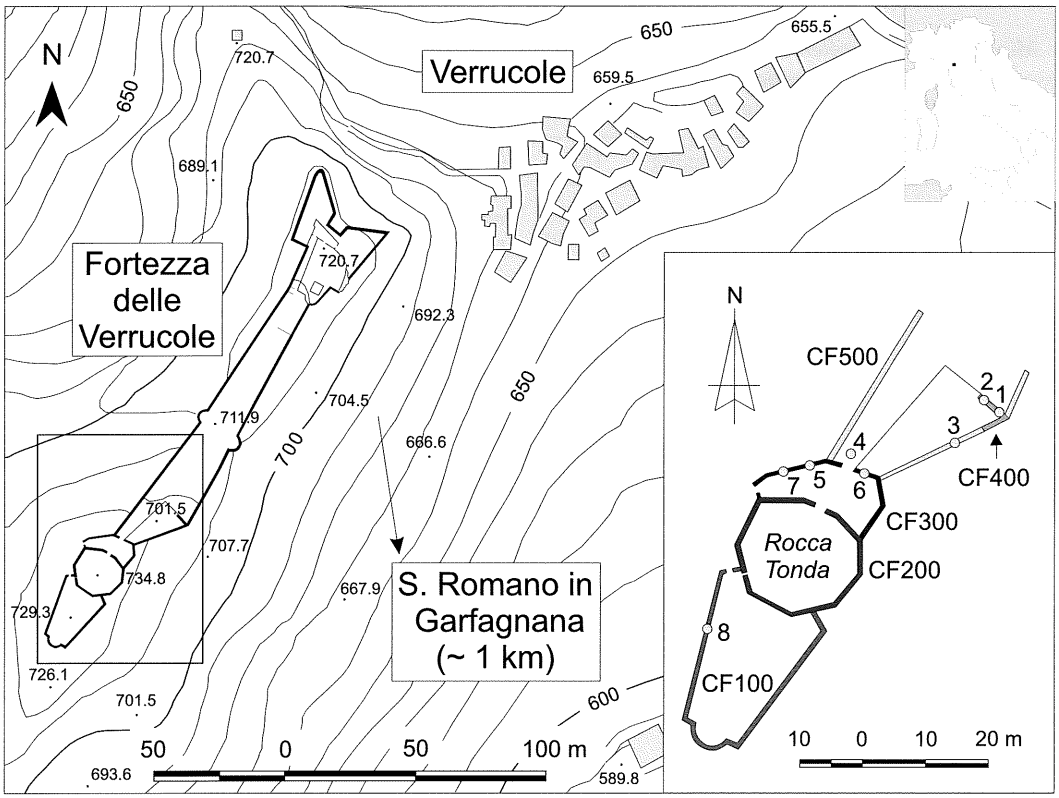

Fig. 1 – Construction drawing of the «Fortezza delle Verrucole» with indication of the sampling places. The building bodies of age pre-Estense (CF200, CF400) and post-Estense (CF100, CF300, CF500) were those indicated by Giovannetti and Notini (1998), on the basis of a late archaeological excavation campaign.

specimens. The parallelepipeds were used to obtain thin polished sections, to measure the physical properties of the mortars and to prepare powder of the bulk specimens and of the lumps. A Zeiss-Axioplane polarising microscope was used to study the thin sections. Chemical analyses of mortar bulk samples were obtained by X-ray fluorescence (XRF), according to the procedure suggested by Franzini *et al.* (1975). CO_2 concentration was determined by a gasometer technique (Leone *et al.*, 1988). X-ray powder diffraction (XRPD) data were collected on bulk mortar samples by means of an automatic diffractometer Philips PW 1830/1710. Thermogravimetric (TG) analyses were obtained on 20 to 30 mg samples, dried at room temperature (silica gel as drying agent) for at least a week, using a simultaneous thermal analyser NETZSCH STA 449C. Powders of the bulk samples as well as of the lumps, hand-selected under the stereomicroscope, were analysed. Morphological features and micro-chemical compositions of binder and lumps were obtained by a scanning electron microscope (Philips XL 20 instrument), equipped with an energy dispersive X-ray analyser (SEM/EDAX). Bulk density (γ_d) was computed as the ratio between the weight of the dry sample and its volume measured by means of a hydrostatic balance on a water-saturated sample. Absolute density (G) was measured on

TABLE 1

Mortar samples collected from the southwest side of the Fortezza delle Verrucole - S. Romano in Garfagnana (LU)

n.	Sample	Place of sampling	H (m)
1	FV-20	6	-0.45
2	FV-07	3	-0.60
3	FV-14	1	1.55
4	FV-13	1	1.20
5	FV-12	1	0.90
6	FV-11	1	0.65
7	FV-01	1	0.60
8	FV-08	3	-0.30
9	FV-15	2	0.70
10	FV-10	7	0.65
11	FV-19	8	0.45
12	FV-03	5	0.35
13	FV-18	2	1.55
14	FV-04	2	1.50
15	FV-17	2	1.45
16	FV-16	2	1.20
17	FV-09	3	0.15
18	FV-06c	4	-0.25
19	FV-06d	4	-0.35
20	FV-06a	4	-0.35
21	FV-06b	4	-0.30

H = height over the local ground level

a fine powder by a He-pycnometer. Water imbibition (W_w), expressed as weight %, was measured according to NorMaL Recommendation 7/81 (1981). Porosity (P) and water saturation index (SI) were computed, respectively, as follows:

$$P\ (\%) = 100 * (1 - \gamma_d / G)$$

$$SI\ (\%) = 100 * W_w * (\gamma_d / \gamma_{H_2O}) / P$$

RESULTS AND DISCUSSION

Varieties and distribution of the masonry stones

The recognised building materials employed in the construction of the FV masonries, are: quartz-feldspars-micas sandstone (80% by volume), and, subordinately, marly and selciferous limestones and some diabases. All these lithotypes belong to the geological formations cropping out in the Garfagnana area (Nardi, 1961; Nardi *et al.*, 1985):

– Macigno: turbidite sandstones (greywackes) with rare and thin pelite interbeds. Oligocene - Lower Miocene;

– Limestones: heterogeneous clayey complex with often sandstones, arenaceous and marly limestones and sometimes shales with marls and thin arenaceous beds. Cretaceous - Eocene;

– Diabase: massive and pillow lavas, sometimes ophiolitic breccias. Upper Jurassic - Cretaceous.

The present-day visible walls of the FV were built up using river pebbles, varying in dimensions from 10 to 40 cm, minor amounts of small limestone blocks, worked using the rock cleavages, and a few diabase fragments, often brecciated and irregular in shape. The pebbles are almost exclusively of sandstone with minor amounts of limestone. They are often broken to obtain a flat surface on the external faces of the walls.

Covering slabs, quoins, blocks worked for lintels of the loopholes, hanging stairs of the main wall, capitals and columns of the internal chapel were also made of Macigno sandstone.

The primary source of sandstone pebbles was the bed of the Serchio River, which flows down to the nearby valley, whereas limestones come from small quarries opened north of studied area, and diabase is from the same site where the FV was built.

Main macroscopic features of the mortars

Table 2 reports the observed macroscopic features of the mortars: colour of the binder, size of the lumps, grain size of the sandy aggregate, presence and quality of gravel fragments, quality of the cut surface. The observed features allow grouping the samples in two groups and into six homogeneous classes.

Group I mortars are characterized by a

TABLE 2

Observed macroscopic features of the mortars

n.	Class	Colour of the binder	Size of the lumps	Grain size of the sandy aggregate	Gravelly fragments	Cutting surface
1	IA	DB*	large	c - m	-	rough
2	IA	DB*	large	c - m	-	rough
3	IB	LC	large	vc - m	baked brick	rough
4	IB	LC	large	c - m	-	smooth
5	IB	LC	large	c - m	-	smooth
6	IB	LC	medium	vc - m	-	rough
7	IB	LC	medium	vc - m	-	rough
8	IB	DC	large	c - m	baked brick	smooth
9	IIA	LB	small	vc - m	limestone	smooth
10	IIA	LB	small	m - f	limestone	smooth
11	IIA	LB	small	m - f	limestone	rough
12	IIA	LB	small	m - f	limestone, coal	smooth
13	IIB	LB	small	c - m	-	smooth
14	IIB	LB	small	vc - m	-	smooth
15	IIB	LB	small	vc - m	-	smooth
16	IIB	LB	small	vc - m	-	smooth
17	IIB	LB	small	c - m	-	smooth
18	IIB	LB	small	m - f	-	smooth
19	IIC	WG	small	m - f	limestone	very smooth
20	IIC	WG	small	m - f	limestone	very smooth
21	IID	GR	small	m - f	pozzolana**	very smooth

* = Lumps are snow-white in colour; ** Pozzolana fragments are about 0.5 mm large. H = distance from the top of the foundations. (LB = light brown; GR = grey-reddish; WG = white-greyish; LC = light cream; DC = dark cream; DB = dark brown; small = < 1 mm; medium = 1-2 mm; large = > 2 mm; vc = very coarse; c = coarse; m = medium; f = fine).

number of large (5 to 10 mm) or medium (2 to 5 mm) sub-spherical lumps, coarse to medium well assorted river sand with rounded to sub-rounded grains, rarely flattened and oriented. Small sub-spherical cavities or bubbles and fractures due to the binder shrinkage are present in all the examined samples. Greater, irregular cavities, partially filled by white calcite concretions, were observed in samples 6 and 7. Class IA mortars have a dark brown binder and a rough cutting surface. Class IB mortars have a binder with a cream colour and a rough to smooth cut surface.

Group II mortars have a binder fairly homogeneous with only few and small (< 1 mm) lumps. Class IIA and IIB mortars have a binder with a light-brown colour and a well assorted sand aggregate with grain size varying from medium-fine to very coarse. Macroscopic porosity is essentially due to several small (< 1 mm) sub-spherical bubbles. The cut surface is smooth. Class IIA mortars contain gravel-size fragments of light brown selciferous and marly limestones lacking in Class IIB mortars. Class IIC mortars differ from the previous one having a white-greyish colour and a medium-fine sand with minor amounts of gravel-size fragments of light brown selciferous and marly limestone. The cut surface of class IIC mortars is very smooth almost polished. Class IID contains only one sample, which is characterized by the presence of about 10% by volume of a reddish natural pozzolana. Other features are similar to those of class IIC mortars. Vitreous and

colourless crystals identified by XRD as Hydrocalumite ($Ca_2Al(OH)_6[Cl_{1-x}(OH)_x].3H_2O$) fill the sub-spherical cavities formed by the shrinkage of the binder.

Mineralogical and petrographic characteristics of the mortars

Table 3 reports the mineralogical compositions (volume percentages) of the mortar samples as determined by modal analysis (no less than 200 points) performed on polished thin sections. The aggregate grains have generally medium to medium-high sphericity and sub-angular to sub-rounded shape. In order of decreasing abundance, they are: mono- or polycrystalline quartz, feldspars (plagioclase prevailing over K-feldspar), lithic fragments (with sedimentary rocks prevailing

TABLE 3

Aggregate mineralogical composition (vol. %) as determined by modal analysis

		Aggregate				Binder								
n.	Class	Q	F	O	R	Total	Inter-granular	Lumps	Total	Pores	L/B	Q/F	Q/R	B/A
1	IA	12.6	9.2	3.3	14.5		38.2	13.3		8.9		1.37	0.87	1.30
2	IA	13.3	9.7	3.2	9.3		49.6	10.5		4.4		1.37	1.43	1.69
1-2		*12.95*	*9.45*	*3.25*	*11.90*	*37.55*	*43.90*	*11.90*	*55.80*	*6.65*	*21.33*	*1.37*	*1.15*	*1.50*
3	IB	18.2	13.6	2.3	23.3		28.4	12.5		1.7		1.34	0.78	0.71
4	IB	13.5	11.8	2.6	14.8		38.1	15.7		3.5		1.14	0.91	1.26
5	IB	10.4	8.3	2.6	17.3		46.7	11.7		3.0		1.25	0.60	1.51
6	IB	13.2	10.1	2.2	18.4		36.8	14.0		5.3		1.31	0.72	1.16
7	IB	10.7	8.5	2.2	18.3		33.5	17.4		9.4		1.26	0.58	1.28
8	IB	13.6	11.4	3.8	18.2*		42.0	4.9		6.1		1.19	0.75	1.00
3-8		*13.27*	*10.62*	*2.62*	*18.38*	*44.89*	*37.58*	*12.70*	*50.28*	*4.83*	*25.26*	*1.25*	*0.72*	*1.15*
9	IIA	14.4	10.4	1.6	9.6		54.4	4.8		4.8		1.38	1.50	1.64
10	IIA	13.8	6.1	1.7	12.9		50.9	3.4		11.2		2.26	1.07	1.57
11	IIA	12.5	6.2	1.1	7.4		55.2	8.5		9.1		2.02	1.69	2.34
12	IIA	11.4	4.5	0.8	6.1		68.2	4.5		4.5		2.53	1.87	3.19
9-12		*13.03*	*6.80*	*1.30*	*9.00*	*30.13*	*57.18*	*5.30*	*62.47*	*7.40*	*8.48*	*2.05*	*1.53*	*2.19*
13	IIB	21.9	9.1	4.3	7.0		49.7	5.9		2.1		2.41	3.13	1.31
14	IIB	14.2	8.2	4.1	10.8		51.2	3.4		8.1		1.73	1.31	1.46
15	IIB	19.3	10.4	2.8	8.2		54.4	2.8		2.1		1.86	2.35	1.41
16	IIB	17.9	10.0	2.6	7.9		54.7	1.6		5.3		1.79	2.27	1.47
17	IIB	18.3	8.0	4.0	10.7		41.6	9.8		7.6		2.29	1.71	1.25
18	IIB	18.6	7.9	3.4	3.5		56.3	1.5		8.8		2.35	5.31	1.73
13-18		*18.37*	*8.93*	*3.53*	*8.02*	*38.85*	*51.32*	*4.17*	*55.48*	*5.67*	*7.51*	*2.07*	*2.68*	*1.44*
19	IIC	18.3	9.8	1.2	15.8		47.5	3.7		3.7		1.87	1.16	1.14
20	IIC	18.4	11.8	2.9	12.5		47.8	1.5		5.1		1.56	1.47	1.08
19-20		*18.35*	*10.80*	*2.05*	*14.15*	*45.35*	*47.65*	*2.60*	*50.25*	*4.40*	*5.17*	*1.72*	*1.32*	*1.11*
21	IID	9.7	4.3	1.1	13.5#	28.60	60.6	0.5	61.10	10.3	0.82	2.26	0.72	2.14

* = brick 1.9%; # = pozzolana 10.3%; Q = quartz; F= feldspars; R = rock fragments; O = other minerals; B = binder; A = aggregate; L = lumps.

on igneous and metamorphic rocks), calcite, phyllosilicates, and heavy minerals (garnet, epidote, titanite, zircon). Residue of natural or artificial pozzolana material was not observed by optical observations neither by scanning electron microscope, except for sample 21 that it is rich (~ 10 % in volume) of small sub-spherical fragments (about 0.5 mm large) of natural pozzolana. The aggregate composition, expressed as quartz (excluding cherts), feldspars (plagioclase and K-feldspar) and rock fragments (excluding carbonates), is shown in Figure 2. The aggregates of the Group I samples plot in a different area, poorer in quartz, than the aggregates of the Group II samples. Sample 21 (Class IID) has an anomalous aggregate composition. On the basis of the classification fields of Tucker (1991) the aggregates of the examined mortars can be classified as arkosic sands and some as intermediate between lithic and arkosic sands.

The binder of the examined mortars shows a non-uniform texture due to the presence of lumps, which in thin section appear as patches devoid of aggregate grains. The lumps are abundant in almost all samples of Group I (sample from 1 to 8) while they are generally scarce in the Group II samples. The (lumps/total binder) ratio has average values equal to 21, 25, 8.5, 7.5, 5.2, 0.8 by volume for the groups IA, IB, IIA, IIB, IIC and IID, respectively. Once again Group I samples differ from Group II samples and sample 21 is anomalous.

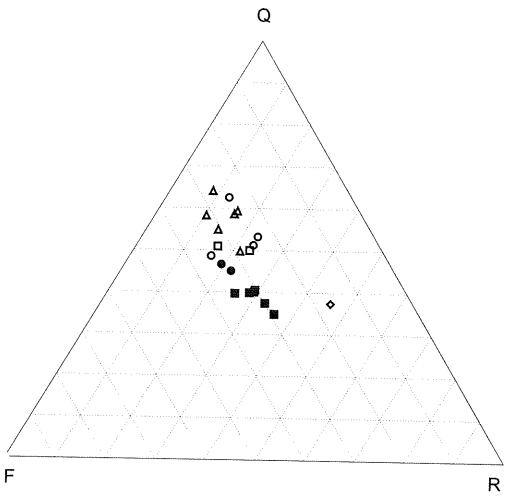

Fig. 2 – Quantitative mineralogical composition (modal composition) of the aggregate fraction. Q = quartz (excluding cherts), F = feldspars (plagioclase and K-feldspar); R = rock fragments (excluding carbonates). ●: samples 1 and 2 (IA); ■: samples from 3 to 8 (IB); ○: samples from 9 to 12 (IIA); △: samples from 13 to 18 (IIB); □: samples 19 and 20 (IIC); ◇: sample 21 (IID).

Optical observations show that the binder is made up of micro- to crypto-crystalline calcite embedded in an isotropic phase. XRPD analyses of some selected lumps from mortar samples belonging to Groups II revealed the presence of prevailing calcite together with varying amounts of a poorly crystalline C-S-H like phase. Small amounts of tetracalcium aluminate 13-hydrate (C_4AH_{13}) and gypsum ($CaSO_4.2H_2O$) were also identified by XRPD on the bulk sample of the mortars 20 and 21.

The binder/aggregate (B/A) ratio average values (last row of Table 3) range from 1.11 to 2.19. No definite trends is evident among the values of the different mortar classes with a possible exception for sample 12 who has the greater measured B/A value.

Chemical characteristics of the mortars

Table 4 reports the chemical compositions determined by X-ray fluorescence and gasometry analyses. The H_2O^+ values have been computed as the difference between the L.O.I. measured by TG analyses and the CO_2 measured by gasometry. The ΔCaO column reports the CaO excess over the quantity needed to saturate all the CO_2 to produce Calcite. The chemical data point out that:

– SiO_2 and CaO are the most abundant chemical components of the examined mortars. They are inversely correlated (r = -0.92, Fig. 3A) and their sum is rather constant in the whole population of samples, from 60 to 68%;

– the ΔCaO, as well as the content of H_2O^+, are too high to be explained by the observed aggregate mineralogy. The positive correlation

TABLE 4

Chemical composition (wt.%) of the bulk mortar samples

n.	Class	H_2O^+	CO_2	Na_2O	MgO	Al_2O_3	SiO_2	P_2O_5	SO3	K_2O	CaO	TiO_2	MnO	Fe_2O_3*SiO_2+CaO	ΔCaO	Alk/Al	Alk/FM	Al/Si
1	IA	3.23	19.60	0.59	2.73	7.31	29.22	0.09	0.02	1.13	31.58	0.42	0.16	3.92	60.80	6.6	0.300	0.233	0.147
2	IA	4.70	18.93	0.32	2.52	7.39	29.63	0.06	0.03	0.92	30.48	0.38	0.26	4.38	60.11	6.4	0.206	0.166	0.147
1-2		*3.97*	*19.27*	*0.46*	*2.63*	*7.35*	*29.43*	*0.08*	*0.03*	*1.03*	*31.03*	*0.40*	*0.21*	*4.15*	*60.46*	*6.5*	*0.253*	*0.200*	*0.147*
3	IB	3.79	12.90	1.06	4.05	9.26	37.18	0.08	0.02	0.86	24.22	0.65	0.15	5.78	61.40	7.8	0.289	0.192	0.147
4	IB	3.96	12.36	1.11	4.54	9.45	37.12	0.10	0.03	0.69	23.91	0.70	0.17	5.86	61.03	8.2	0.272	0.169	0.150
5	IB	5.05	9.90	0.65	3.36	9.51	40.35	0.08	0.04	1.08	23.94	0.55	0.17	5.32	64.29	11.3	0.235	0.188	0.139
6	IB	3.44	13.86	0.88	3.57	8.92	37.29	0.08	0.02	0.92	24.97	0.58	0.17	5.30	62.26	7.3	0.274	0.197	0.141
7	IB	3.56	14.50	0.85	3.33	8.64	36.72	0.08	0.02	0.94	25.55	0.54	0.18	5.09	62.27	7.1	0.280	0.207	0.139
8	IB	5.67	8.77	0.44	3.35	8.75	39.20	0.08	0.07	0.92	25.75	0.46	0.30	6.24	64.95	14.6	0.197	0.138	0.132
3-8		*4.25*	*12.05*	*0.83*	*3.70*	*9.09*	*37.98*	*0.08*	*0.03*	*0.90*	*24.72*	*0.58*	*0.19*	*5.60*	*62.70*	*9.4*	*0.258*	*0.182*	*0.141*
9	IIA	4.30	9.50	0.66	2.72	10.00	48.71	0.08	0.03	1.50	17.89	0.38	0.22	4.01	66.60	5.8	0.271	0.287	0.121
10	IIA	5.00	14.35	0.54	2.89	7.84	33.37	0.08	0.04	0.98	30.29	0.39	0.22	4.01	63.66	12.0	0.249	0.197	0.138
11	IIA	4.68	12.14	0.49	2.69	8.45	35.89	0.14	0.05	0.99	28.30	0.38	0.32	5.48	64.19	12.8	0.222	0.182	0.139
12	IIA	5.43	18.76	0.14	2.24	5.63	25.77	0.02	0.08	0.56	37.60	0.24	0.26	3.27	63.37	13.7	0.149	0.108	0.129
9-12		*4.85*	*13.69*	*0.46*	*2.64*	*7.98*	*35.94*	*0.08*	*0.05*	*1.01*	*28.52*	*0.35*	*0.26*	*4.19*	*64.46*	*11.1*	*0.223*	*0.194*	*0.132*
13	IIB	5.78	7.99	0.42	2.59	9.32	43.32	0.07	0.04	1.29	24.61	0.35	0.27	3.95	67.93	14.4	0.224	0.230	0.127
14	IIB	4.89	9.56	0.56	2.64	9.54	44.21	0.08	0.03	1.37	22.46	0.40	0.24	4.02	66.67	10.3	0.252	0.260	0.127
15	IIB	4.40	10.04	0.56	3.32	9.86	43.51	0.07	0.03	1.45	22.16	0.37	0.23	4.00	65.67	9.4	0.253	0.227	0.134
16	IIB	4.36	9.17	0.58	2.85	10.47	45.25	0.08	0.03	1.50	20.87	0.38	0.27	4.19	66.12	9.2	0.246	0.261	0.136
17	IIB	3.86	11.08	0.75	2.75	9.77	46.50	0.10	0.03	1.76	19.28	0.38	0.19	3.55	65.78	5.2	0.321	0.340	0.124
18	IIB	5.22	9.22	0.50	2.49	9.35	44.00	0.13	0.03	1.33	23.14	0.36	0.25	3.98	67.14	11.4	0.242	0.256	0.125
13-18		*4.75*	*9.51*	*0.56*	*2.77*	*9.72*	*44.47*	*0.09*	*0.03*	*1.45*	*22.09*	*0.37*	*0.24*	*3.95*	*66.55*	*10.0*	*0.256*	*0.262*	*0.129*
19	IIC	4.92	10.48	0.61	2.33	7.41	38.88	0.12	0.05	1.02	29.29	0.34	0.19	4.36	68.17	16.0	0.284	0.243	0.112
20	IIC	6.72	8.52	0.46	2.62	7.86	36.02	0.11	0.05	0.92	31.52	0.39	0.22	4.59	67.54	20.7	0.223	0.183	0.129
19-20		*5.82*	*9.50*	*0.54*	*2.48*	*7.64*	*37.45*	*0.12*	*0.05*	*0.97*	*30.41*	*0.37*	*0.21*	*4.48*	*67.86*	*18.4*	*0.254*	*0.213*	*0.121*
21	IID	5.76	13.12	0.64	2.63	8.31	33.42	0.21	0.04	0.86	29.47	0.46	0.21	4.87	62.89	12.8	0.239	0.203	0.147

*Fe_2O_3 = total iron expressed as Fe_2O_3; ΔCaO = CaO excess over the quantity required to saturate the CO_2 to produce calcite; Alk = molar (Na_2O + K_2O); FM = molar (Fe_2O_3 + MgO); Al = molar Al_2O_3; Si = molar SiO_2.

(r = 0.87, Fig. 3B) between the ΔCaO and the H_2O^+ content suggests that the greater part of these components must be present in the binder as an amorphous or poorly crystallized phase.

– the sulphur content, given as SO_3 in Table 4, is low in all the examined samples. It may be present as gypsum, formed by the percolation of polluted rainwater into the masonries, or as pyrite in the rock fragments of the aggregate.

– no substantial differences exist among the chemical compositions of the examined samples. Only the average values exhibit minor differences: Group I samples have somewhat smaller values of H_2O^+, SiO_2+CaO and ΔCaO than the Group II samples.

Table 5 reports, for the six classes of mortars, the average chemical compositions obtained by SEM/EDAX analyser on small

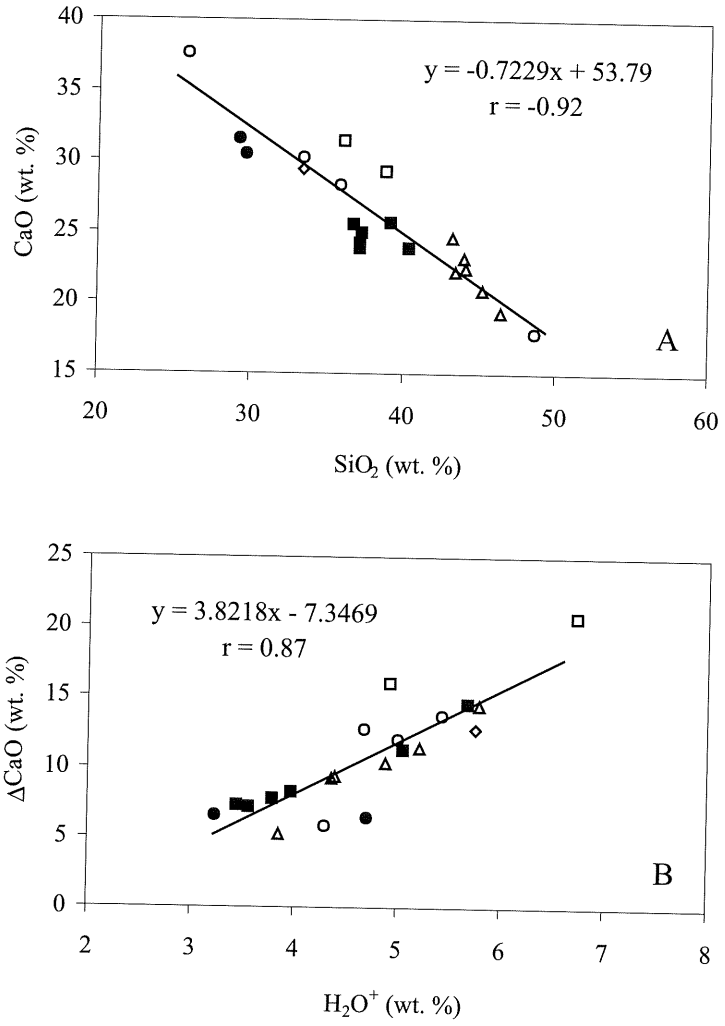

Fig. 3 - Equations of linear regression between some components of the mortars. ●: samples 1 and 2 (IA); ■: samples from 3 to 8 (IB); ○: samples from 9 to 12 (IIA); △: samples from 13 to 18 (IIB); □: samples 19 and 20 (IIC); ◇: sample 21 (IID).

TABLE 5

Average chemical compositions (wt.%) of the mortar binder

Classes	Group I			Group II		
	IA (n=8)	IB (n=28)	IIA (n=28)	IIB (n=44)	IIC (n=11)	IID (n=7)
	Aver. $(\sigma)_j$	Aver. $(\sigma)_j$	Aver. $(\sigma)_j$	Aver. $(\sigma)_j$	Aver. $(\sigma)_j$	Aver. $(\sigma)_j$
Na_2O	0.27 ± 0.32	0.30 ± 0.32	0.24 ± 0.23	0.42 ± 0.36	0.25 ± 0.30	0.30 ± 0.34
MgO	1.36 ± 1.04	1.27 ± 0.94	1.91 ± 1.25	1.78 ± 1.10	1.01 ± 0.75	1.52 ± 1.01
Al_2O_3	3.46 ± 1.67	7.09 ± 1.69	7.75 ± 1.17	8.58 ± 0.85	4.70 ± 1.16	9.19 ± 6.17
SiO_2	9.74 ± 4.78	43.70 ± 6.50	42.93 ± 4.37	48.17 ± 3.19	36.98 ± 3.98	27.08 ± 6.30
SO_3	0.40 ± 0.25	0.40 ± 0.25	0.63 ± 0.27	0.45 ± 0.25	0.57 ± 0.43	0.53 ± 0.20
K_2O	0.53 ± 0.19	0.43 ± 0.21	0.31 ± 0.28	0.39 ± 0.19	0.37 ± 0.10	0.50 ± 0.12
CaO	82.93 ± 5.94	45.10 ± 8.40	45.13 ± 5.08	38.79 ± 3.94	54.66 ± 3.46	59.59 ± 3.44
Fe_2O_3	1.31 ± 0.37	1.71 ± 0.69	1.10 ± 0.50	1.42 ± 0.51	1.46 ± 0.52	1.29 ± 0.59
i	0.2	1.1	1.1	1.4	0.8	0.6
Alk/Al	0.294	0.135	0.094	0.130	0.173	0.113
Alk/FM	0.398	0.355	0.234	0.352	0.367	0.377
Al/Si	0.419	0.191	0.213	0.210	0.150	0.400

n = number of analysis; i = $(SiO_2 + Al_2O_3 + Fe_2O_3)$ / (CaO + MgO); Alk = molar (Na + K); Al = molar Al; FM = molar (Fe + Mg); Si = molar Si.

areas (5-20 μm^2) of the binder. Substantial micro-chemical variations result among the samples belonging to the same group as suggested by the high standard deviations $(\sigma)_j$ values reported in Table 5. From the SEM/EDAX analyses three group of mortars can be distinguished: Class IA mortars with high CaO content and high Alk/Al and Al/Si ratio values, Sample 21 (Class II D) mortar with medium CaO content, high Al/Si ratio value, low Alk/Al ratio value, and the remaining (Classes IB, IIA, IIB, IIC) mortars with low CaO content and low Alk/Al and Al/Si ratio values.

Figure 4 shows the relation among the major chemical compounds (CaO, SiO_2 and Al_2O_3) of the binders. It appears that the binder compositions are highly variable, ranging from an air-hardening lime (samples 1 and 2 that plot close to the CaO corner) to hydraulic limes. Several samples plot near the middle point of the segment tying CaO and SiO_2 compounds.

The high SiO_2 content of the binders must be ascribe to several causes such as: loss of calcium oxide due to weathering processes, presence in the filler of a fine SiO_2-rich fraction (i.e. clayey and/or muddy materials), increasing of SiO_2 or decreasing of CaO contents due to the reactions between binder and aggregate fractions and addition during the manufacturing process of a prevailing silica-rich material. Examining closely the collected data, some hypothesis can be evaluated. For example, the only CaO loss ascribed to weathering process or, generally, to reacting free-calcium hydroxide is contrasting with the consideration that not all the mortar samples are likewise exposed to weathering process, and that no reacting edge, around reactive grains, are observed in the studied mortars by optical microscope nor by SEM/EDAX observations. Furthermore, a loss of material would increase the porosity of the mortars and, therefore, decrease their mechanical properties, in apparent contrast with the experimental data.

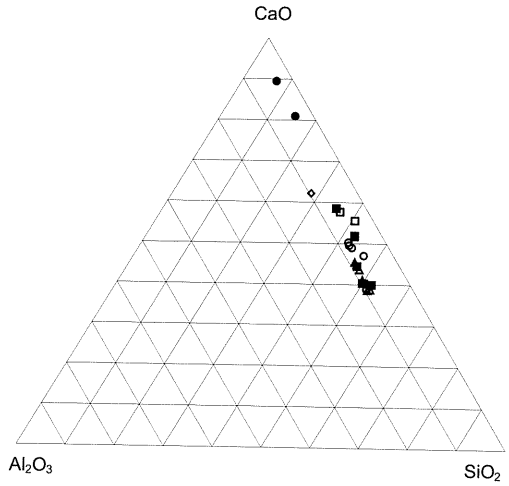

Fig. 4 - Major chemical components of the mortar binder determined by SEM/EDAX analyses. ●: samples 1 and 2 (IA); ■: samples from 3 to 8 (IB); ○: samples from 9 to 12 (IIA); △: samples from 13 to 18 (IIB); □: samples 19 and 20 (IIC); ◇: sample 21 (IID).

Therefore, if not assuming as fundamental reason the degradation processes or the chemical processes among reactive aggregate grains and calcium hydroxide belonging to the binder fraction, the micro-chemical data show that a fine silica-rich fraction, e.g. a natural or artificial pozzolana material or more simply a very fine amount of aggregate fraction, must be intimately mixed with the mortar binder.

Physical properties of the mortars

Table 6 reports the measured and calculated values of the main physical properties of the examined mortars. The absolute densities of the mortar samples (G) range from 2.51 g/cm^3 (samples 19 and 20) to 2.67 g/cm^3 (sample 1). The great differences among the measured absolute density values are not easily explained as due to variable binder/aggregate ratios. The more abundant aggregate minerals have in fact absolute densities ranging from about 2.65 g/cm^3, for quartz and plagioclases, to 2.71 g/cm^3 for calcite. Absolute density values, similar to those given in Table 6, were measured by Franzini *et al.* (2000a; 2000b) in the mortars of the Leaning Tower of Pisa. These low G values were imputed to the presence in the binders of amorphous C-S-H compounds, which have densities ranging from 2.22 to 2.35 g/cm^3 (Taylor, 1972). The same explanation seems true also for the mortars of Group II samples and, perhaps, for the mortars of the Class IB samples. To strengthen this conclusion we observe that a negative correlation exists between the H_2O^+ content (Table 4) and the G values (Table 6).

Water imbibition by weight (W_w) values vary from 19.5 to 47 %. The porosity values (P) range from 34 to 54%, without any difference among samples pertaining to the different classes. Also the index of water saturation (SI) is fairly constant in all examined mortars and its average value next to 100% point out that the water fills all the voids of the samples.

Conclusions

The chemical, mineralogical, petrographic and physical data collected on the mortars from the walls of the southwest side of the «Fortezza delle Verrucole - S. Romano in Garfagnana (LU)» has allowed to characterize their binder and aggregate fractions as well as to individuate the main typologies of employed mixtures.

The macroscopic features of the sample surfaces have allowed to group the 21 collected samples in two Groups and six Classes.

Class IID contain only one sample, the sample number 21. This sample is different from all the other samples in respect to all its properties.

The optical study of polished thin sections has revealed (Fig. 2) that the aggregate composition of Group I samples is different from that of the Group II samples. The same subdivision is pointed out by the values of the absolute density that are greater for Group I samples than for Group II samples.

The micro-chemical data directly obtained

TABLE 6

Main physical properties of the mortars

Sample	Class	G (g/cm³)	γ_d (g/cm³)	Ww (%)	P (%)	SI (%)
1	IA	2.67	1.58	24.7	40.8	96
2	IA	2.66	1.41	31.1	47.0	93
1-2		*2.67*	*1.50*	*27.9*	*43.9*	*95*
3	IB	2.64	1.74	19.5	34.1	99
4	IB	2.63	1.54	26.4	41.4	98
5	IB	2.59	1.60	23.9	38.2	100
6	IB	2.63	1.59	24.7	39.5	99
7	IB	2.64	1.72	20.4	34.8	100
8	IB	2.58	1.39	33.3	46.1	100
3-8		*2.62*	*1.60*	*24.7*	*39.0*	*99*
9	IIA	2.57	1.42	29.8	44.7	95
10	IIA	2.56	1.37	32.6	46.5	96
11	IIA	2.59	1.37	33.6	47.1	98
12	IIA	2.55	1.16	47.0	54.5	100
9-12		*2.57*	*1.33*	*35.8*	*48.2*	*97*
13	IIB	2.55	1.38	31.5	45.9	95
14	IIB	2.56	1.48	27.4	42.2	96
15	IIB	2.56	1.65	20.4	35.5	94
16	IIB	2.57	1.45	28.1	43.6	93
17	IIB	2.58	1.55	22.7	39.9	88
18	IIB	2.55	1.39	31.2	45.5	95
13-18		*2.56*	*1.48*	*26.9*	*42.1*	*94*
19	IIC	2.51	1.56	24.0	37.8	99
20	IIC	2.51	1.58	20.7	37.1	88
19-20		*2.51*	*1.57*	*22.4*	*37.5*	*94*
21	IID	2.57	1.43	30.8	44.4	99

G, γ_d = absolute and bulk density, respectively; W_w = water imbibition; P = porosity; SI = index of water saturation.

on the binder fraction of the bulk mortar sample, together with XRPD and TG analyses, indicate a clear difference between the Class IA samples and all the other samples.

On the basis of the recognized macroscopic typologies of mortars and of their measured properties, at least two different constructive phases were found. They are:

Ancient phase: In this phase air-hardening (Class IA) or hydraulic (Class IB) lime mortars, produced with typically ancient technology by mixing lime putty and locally available river sand, are employed. These mortars are easily recognizable for the presence from large to medium lumps due to a not complete mixing of binder and aggregate. Besides, their aggregate is constituted by coarse well-sorted Serchio River sand, in which it is possible to recognised fragments of locally exposed rocks. The mortar samples belonging to this ancient phase came from structures of the zone 1, 3 and 6, where the archaeological excavations were opened (with exception of the sample 17 that undoubtedly belongs to the following phase owing to its modern techniques of production).

Recent phase: all the others sampled mortars belong to this phase and they came from the visible building structures sampled in the zones 4, 5, 7 and 8 or that were bring up to the light from the archaeological excavations such as those from the zone 2 and 3 (only the sample 17) (Fig. 1). They are hydraulic lime mortars or cement mortars, produced with a modern technology, in which it is frequently possible to find gravely fragments made up of silicatic and carbonate rocks. It seems, therefore, that the recent phase could be not too ancient.

In brief, the collected data group the twenty-one examined samples by six homogeneous classes from the macroscopic point of view and by two types of mortars on the basis of the chemical and mineralogical characteristics of the binder and aggregate fractions consisting of hydraulic binders prevailing on air-hardening binder and of coarse-medium river sands, respectively.

ACKNOWLEDGMENTS

The author wishes to thank Maurizia Adriani of the Soprintendenza B.A.P.P.S.A.D. di Pisa, Livorno, Lucca e Massa Carrara, executive manager of the restoration project, for her permission to publish this work. Thanks are also due to Prof. Marco Franzini of the Dipartimento di Scienze della Terra - Università di Pisa, for his critical review of the manuscript. This work has been financially supported by the Italian National Research Council (CNR) - Progetto Finalizzato Beni Culturali.

REFERENCES

DE ANGELI N., GIOVANETTI L., NOTINI P., PASOGLI TACCA G., PREITE M. and RANDELLI A. (1998) — *La Fortezza di Verrucole*. Pezzini, Viareggio, Italy, 300 pp.

FRANZINI M., LEONI L. and LEZZERINI M. (2000a) — *A procedure for determining the chemical composition of binder and aggregate in ancient mortars: its application to mortars from some medieval buildings in Pisa*. J. Cult. Heritage, **1**, 365-373.

FRANZINI M., LEONI L., LEZZERINI M. and SARTORI F. (2000b) — *The mortar of the «Leaning Tower» of Pisa: the product of a medieval technique for preparing high-strength mortars*. Eur. J. Mineral., **12**, 1151-1163.

FRANZINI M., LEONI L. and SAITTA M. (1975) — *Revisione di una metodologia analitica per fluorescenza X, basata sulla correzione completa degli effetti di matrice*. Rend. Soc. It. Miner. Petrol., **31**, 365-378.

GIOVANETTI L. and NOTINI P. (1998) — *Dati preliminari sui corpi di fabbrica della Fortezza delle Verrucole*. In: *La Fortezza di Verrucole*. Pezzini, ed., Viareggio, Italy, 95-113.

LEONE G., LEONI L. and SARTORI F. (1988) — *Revisione di un metodo gasometrico per la determinazione di calcite e dolomite*. Atti Soc. Tosc. Sc. Nat., Mem., Serie A, **95**, 7-20.

NARDI R. (1961) — *Geologia della zona tra la Pania della Croce, Gallicano e Castelnuovo di Garfagnana (Alpi Apuane)*. Boll. Soc. Geol. It., **80**, 257-334.

NARDI R., POCHINI A., PUCCINELLI A., TRIVELLINI M. and D'AMATO AVANZI G. (1985) — *Valutazione del rischio da frana in Garfagnana e nella media valle del Serchio (Lucca)*. 1) Carta geologica e carta della franosità degli elementi «Gragnana», «Piazza al Serchio», «Casciana» e «Ceserana» (Scala 1:10000). Boll. Soc. Geol. It, **104**, 585-599.

NORMAL RECOMMENDATION 7/81 (1981) — *Assorbimento d'acqua per immersione totale - Capacità d'imbibizione*. CNR – ICR, Roma.

TAYLOR H.F.W. (1972) — *Appendix 1. Tabulated Crystallographic Data*. In: *The chemistry of cements*. Volume 2. H.F.W. Taylor, ed., Academic Press, London, 347-403.

TUKER M.E. (1991) — *Sedimentary petrology*. Blackwell, Oxford, 260 pp.